

# Phoresis in turbulent flows

Vishwanath Shukla<sup>1,2</sup>, Romain Volk<sup>1</sup>, Mickaël Bourgoin<sup>1</sup> and  
Alain Pumir<sup>1</sup>

<sup>1</sup> Laboratoire de Physique, ENS de Lyon, UMR CNRS 5672, Université de Lyon,  
France

<sup>2</sup> Service de Physique de l'Etat Condensé, Université Paris-Saclay, CEA Saclay,  
91191 Gif-sur-Yvette, France

E-mail: [research.vishwanath@gmail.com](mailto:research.vishwanath@gmail.com), [romain.volk@ens-lyon.fr](mailto:romain.volk@ens-lyon.fr),  
[mickael.bourgoin@ens-lyon.fr](mailto:mickael.bourgoin@ens-lyon.fr), [alain.pumir@ens-lyon.fr](mailto:alain.pumir@ens-lyon.fr)

**Abstract.** Phoresis, the drift of particles induced by scalar gradients in a flow, can result in an effective compressibility, bringing together or repelling particles from each other. Here, we ask whether this effect can affect the transport of particles in a turbulent flow. To this end, we study how the dispersion of a cloud of phoretic particles is modified when injected in the flow, together with a blob of scalar, whose effect is to transiently bring particles together, or push them away from the center of the blob. The resulting phoretic effect can be quantified by a single dimensionless number. Phenomenological considerations lead to simple predictions for the mean separation between particles, which are consistent with results of direct numerical simulations. Using the numerical results presented here, as well as those from previous studies, we discuss quantitatively the experimental consequences of this work and the possible impact of such phoretic mechanisms in natural systems.

*keywords:* turbulence; turbulent transport; phoresis; direct numerical simulations

## 1. Introduction

The transport of particles and macro-molecules in a flow can be strongly affected by a scalar quantity present in the fluid. The phenomenon of phoresis investigated here results from a drift velocity of the particles,  $\mathbf{v}_d$ , proportional to the gradient of a scalar quantity,  $\theta(\mathbf{x}, t)$  :  $\mathbf{v}_d = \alpha \nabla \theta(\mathbf{x}, t)$ . The scalar field involved could be temperature (thermophoresis), a chemical species (chemophoresis), or salt concentration (diffusiophoresis). The magnitude and sign of the phoretic mobility coefficient  $\alpha$  depends on the nature of the interaction of the particle with the scalar field [1]. Electrophoresis and magnetophoresis [2, 3], induced by a drift proportional to the electric or magnetic field, respectively, provide two extra examples of phoresis with potential practical utility.

It is well-known that the diffusive transport of particles and of macro-molecules in a laminar flow is generally very slow because of their very small intrinsic molecular diffusion coefficient. Recent studies show that a significant enhancement of the transport properties can be achieved by addition of a small salt concentration to the solution, which induces a phoretic mobility in response to the salt gradients [4, 5]. The enhanced mobility of the colloids observed in microfluidic channel experiments with salt gradients [4, 5] was initially interpreted in terms of an effective diffusion aided by diffusiophoresis. The inferred diffusion coefficient is larger than what is expected from a simple Brownian motion of colloidal particles and for certain salts it is almost two orders of magnitude larger. This makes diffusiophoresis an important concept with a practical utility, which can be used to selectively control the mobility of colloids or macro-molecules in microfluidic devices for scientific and/or industrial purposes. Similar arguments based on effective diffusivity were later used to explain the experimental results on enhanced or delayed mixing of colloids in chaotic flows [6].

However, more recent studies [7, 8] showed that a description of these phenomena in terms of a modulated diffusion coefficient does not capture all the physics at play. In particular, it fails to explain the evolution in space and time of the colloids concentration, especially mixing and de-mixing at short times.

These studies stressed the importance of the effective *compressibility* of the velocity field  $\mathbf{v}$  seen by the particles:  $\nabla \cdot \mathbf{v} \neq 0$ . Numerical simulations and experiments employing diffusiophoresis in chaotic flows have conclusively shown that the compressibility strongly affects the transport of particles. In particular, it was found that the compressible nature of the velocity field acts as a source of colloids concentration variance [7]. As a consequence the whole mixing process is modified by the phoretic transport, leading to either mixing or de-mixing depending on the local environment. Moreover recent experiments in a chaotic flow clearly demonstrated that diffusiophoresis modifies the properties of the particle distribution not only at small-scales, but even at the largest scales of the mixing process [8].

Here, we ask how the transport of colloids by a turbulent flow is affected by phoresis. Turbulent motion in fluids involves a wide range of length and time scales and is known to enhance mixing by generating strong gradients of advected scalar fields. The study

of the transport of particulate matter in turbulent flows is an important problem, with far reaching implications for a wide spectrum of applications, such as rain initiation in warm clouds [9] or controlling industrial flows [10]. The velocity field experienced by inertial particles, with a finite-size and/or different density compared to the carrier fluid, is compressible [11, 12]. It is known that this effective compressibility results in an inhomogeneous distribution of inertial particles [13, 14, 15] in contrast to the homogeneous distribution of pure tracer particles in turbulent flows. Therefore, it is natural to use the concepts and current understandings of the role played by the effective compressibility in turbulent transport processes, when extended to phoretic particles driven by turbulent scalar field [16, 17, 18, 19].

In the following, we examine the consequences of the turbulent fluctuations on the dynamics of a cloud of particles undergoing phoresis. In the spirit of the original experiments, documenting phoretic effects by injecting locally colloids and salt [4, 5], we focus on the effect of phoretic compressibility at short times, after releasing a cloud of salt and colloids, of characteristic size  $\ell_c$ , in a turbulent flow. Although it is transported by a turbulent flow, such a cloud of size  $\ell_c$  will grow ballistically during a characteristic time  $t_c$ , which can be estimated using the standard phenomenological description of turbulence (see Section 3, and ref. [20]).

Dimensionally, the effective compressibility  $(\nabla \cdot \mathbf{v})$ , where  $\mathbf{v}$  is the velocity seen by the particles, is an inverse time scale, which should be compared to the typical time scale of the motion; note that  $\mathbf{v}$  includes both the velocity of the carrier flow  $\mathbf{u}$  and the phoretic drift  $\mathbf{v}_d$ . Therefore, we introduce a dimensionless number,  $\Phi_c \sim (\nabla \cdot \mathbf{v}) \times t_c$ , which characterizes the competition between turbulent dispersion and compressibility. We use these phenomenological arguments, which are corroborated by Direct Numerical Simulations (DNS) of the Navier-Stokes equations (NSE), to show that  $\Phi_c$  is the parameter which controls the mixing of the phoretic particles in this problem. In particular, we show that the maximum contraction of the particle cloud occurs in the ballistic regime of turbulent dispersion, and varies as  $\exp(-\gamma\Phi_c)$ . Our results show that  $\gamma$  has similar values for different Reynolds numbers and particle cloud sizes, thereby suggesting an universal behavior.

Phoretic effects have also been observed to play a role in randomly stirred chaotic flows in two dimensions (2D) [7], in a regime where the scalar field is in a statistically stationary state. We discuss the expression of  $\Phi_c$  in such cases. Our estimates, obtained by using realistic values of the physical parameters, suggest that phoretic effects should also be observable in turbulent flows in steady state configuration at very small scales.

## 2. Methods

Specifically, we consider here a simple problem, whereby a blob of scalar field with a simple Gaussian profile is released in a turbulent fluid, along with a cloud of particles, as illustrated in figure 1. The scalar field decays, as it is mixed by the turbulence. During this process, strong scalar gradients develop and this drives the phoretic motion of the

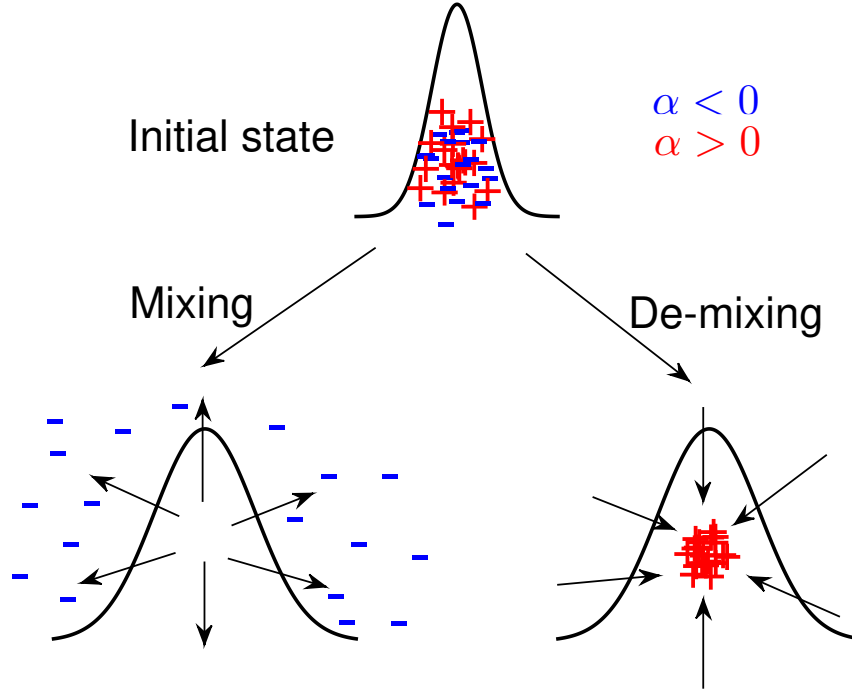


**Figure 1. Turbulent phoresis.** Schematic diagram showing the initial configuration of the scalar field and the resulting phoretic motion of the colloids. Particles with positive ( $\alpha > 0$ , red “+” symbol) and negative ( $\alpha < 0$ , blue “-” symbol) phoretic mobilities are initially distributed in a Gaussian blob of scalar field (upper narrow Gaussian profile). Scalar mixing in a turbulent fluid is indicated by drawing a broader scalar profile; depending on the sign of the phoretic mobility  $\alpha$ , the particles either tend to cluster (de-mixing) or separate from each other (mixing).

particles. We stress that this configuration is experimentally realizable, for example in a turbulent jet or a water-tunnel, where the statistical properties of the cloud of particles and their dispersion could be accurately measured. We assume here that the flow is incompressible, so that its description is based on the (NSE)

$$\frac{\partial \mathbf{u}}{\partial t} + (\mathbf{u} \cdot \nabla) \mathbf{u} = -\nabla p + \nu \nabla^2 \mathbf{u} + \mathbf{f} \quad (1)$$

where  $\nabla \cdot \mathbf{u} = 0$  imposes the incompressibility condition on the three-dimensional (3D) velocity field  $\mathbf{u}$ .  $p$  is the pressure field,  $\nu$  is the fluid viscosity and  $\mathbf{f}$  is the forcing term, acting at large scales, which maintains the turbulent flow statistically stationary. The spatio-temporal evolution of the scalar field fluctuations  $\theta(\mathbf{x}, t)$  is governed by the advection-diffusion equation

$$\frac{\partial \theta}{\partial t} + (\mathbf{u} \cdot \nabla) \theta = \kappa \nabla^2 \theta, \quad (2)$$

where  $\kappa$  is the diffusion coefficient of the scalar field constituents, whose spatial average  $\langle \theta \rangle_{\text{spatial}}$  is zero. We furthermore assume that the molecular diffusion coefficient of the colloidal particles of interest here is orders of magnitude smaller than the constituents of the scalar field. Therefore, we are interested in the limiting case where the particles

are advected by the combined velocity field of the turbulent flow  $\mathbf{u}$  and the phoretic contribution  $\mathbf{v}_d = \alpha \nabla \theta$ ,  $\alpha$  being the phoretic mobility coefficient, quantifying the efficiency of the gradient to generate an additional drift motion for the particles. To study the dynamics of this assembly of discrete particles undergoing phoresis in a turbulent environment, we adopt a Lagrangian framework, in which the velocity of a particle, labelled by the index  $i$ , and located at position  $\mathbf{X}_i(t)$  is given by

$$\mathbf{v}_i = \mathbf{u}(\mathbf{X}_i, t) + \alpha \nabla \theta(\mathbf{X}_i, t), \quad (3)$$

where  $d\mathbf{X}_i/dt = \mathbf{v}_i$ .

As briefly sketched in the previous section, the phenomenological approach of particle dynamics used here is based on the standard (Kolmogorov-Obukhov) phenomenological description of turbulence [20]. A three-dimensional (3D) turbulent flow is sustained by injecting energy at a rate  $\varepsilon$  per unit mass, at the large length scales,  $\ell \sim L_0$ , comparable to the system size. This energy is transferred to smaller length scales, down to the scale  $\eta$  where energy is dissipated by viscosity:  $\eta = (\nu^3/\varepsilon)^{1/4}$ . The range of scales, defined by  $\eta \ll \ell \ll L_0$ , is defined as the inertial scales. The transfer of energy is a result of the nonlinear interactions, represented by the advection term in the NSE (1). An (almost) self-similar structure is often postulated over the inertial range of scales, which is characterized by a constant flux of energy,  $\varepsilon$  [20].

We test our phenomenological arguments and make them more quantitative by numerically determining the statistical properties of this system. To this end, we perform DNSs of the NSE (1) and the advection-diffusion equations (2) in 3D to determine the fluid velocity field  $\mathbf{u}$  and the scalar field  $\theta$ , respectively; we then use them to numerically determine the trajectories of the particles. We solve the NSE in a triply-periodic domain by using the pseudospectral code, as described, e.g. in Refs. [21, 15]. The flow is maintained statistically stationary by forcing the velocity field at large scales (small wave numbers  $k$ ) [21]. Simulations were carried out at moderate resolutions, with  $96^3$ ,  $192^3$  and  $384^3$  Fourier modes. Adequate spatial resolution for the velocity field was imposed, by maintaining the product  $k_{max}\eta \geq 1.5$ . This allowed us to simulate flows up to a Taylor-scale Reynolds number  $R_\lambda = 175$ . To address the more demanding resolution criteria for the scalar field [21], we work here with a dimensionless ratio  $\nu/\kappa$  equal to  $1/2$ . We refer here to this dimensionless ratio as the Prandtl number  $Pr$ , a terminology which is generally used when for a scalar field (the corresponding dimensionless ratio is known as the Schmidt number,  $Sc$ , in the case of a concentration field).

Here, we start with an initial configuration, where we release in a turbulent flow a Gaussian blob of scalar:

$$\theta(\mathbf{x}, t = 0) = \theta_0 \exp\left(-\frac{\mathbf{x}^2}{2\ell_c^2}\right) \quad (4)$$

containing 2000 particles which are randomly distributed within it with the same Gaussian distribution. The size  $\ell_c$  then serves as a convenient measure both of the scalar blob and the particle cloud. The effect of the scalar is to attract particles close to the center when  $\alpha\theta_0 > 0$ , and repel them away from the center when  $\alpha\theta_0 < 0$ , as illustrated in figure 1.

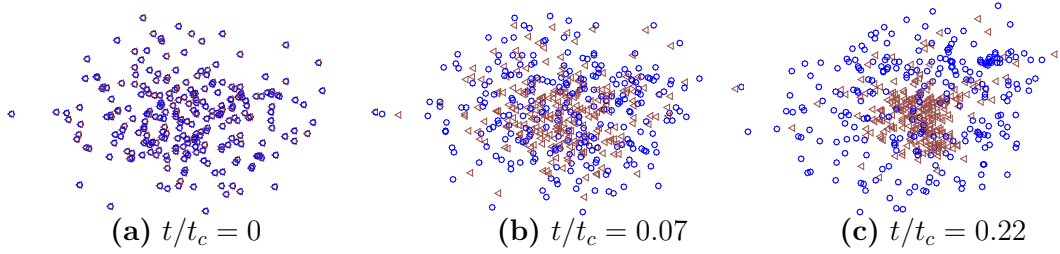


**Figure 2. Mixing/de-mixing of phoretic particles.** Positions of two particle types at three different times:  $t/t_c = 0$  (a),  $t/t_c = 0.07$  (b), and  $t/t_c = 0.22$  (c). The particles correspond to two different values of the dimensionless number  $\Phi_C = -5.81$  (blue circles) and  $\Phi_C = 5.81$  (brown triangles) to same local environment, from the DNS run with  $R_\lambda = 95$  and  $\ell_c/\eta = 20.8$ . The particles with  $\Phi_C > 0$  de-mix, whereas the ones with  $\Phi_C < 0$  undergo enhanced mixing, for a scalar blob with the Gaussian profile in a turbulent flow.

A list of the simulations carried out in this work is provided in Table A1 and Table A2, see Appendix A.

### 3. Results

#### 3.1. Competition between phoretic effects and turbulence mixing

As already stressed, the velocity field seen by the particles, (3), is compressible and its divergence is proportional to the Laplacian of the scalar field  $\nabla \cdot \mathbf{v} = \alpha \nabla^2 \theta$ . The divergence field  $\mathcal{C}(\mathbf{x}, t) \equiv \nabla \cdot \mathbf{v}$  can serve as a local indicator of the compressibility. With (4) as the initial condition for the scalar field, the initial compressibility is given by  $\mathcal{C}_0 \sim \alpha \theta_0 / \ell_c^2$ . Starting from initial condition, the blob of fluid which contains both scalar and particles will be advected by turbulent motions. Particles will then experience compressible effects at the scale  $\ell_c$  (of the order  $\mathcal{C}_0$ ), until the scalar field is distorted, which is achieved in a time  $t_c$  corresponding to the eddy turnover time at scale  $\ell_c$ . Such a time scale can be estimated following standard phenomenology of turbulent flows [20]. As  $\ell_c$  lies in the inertial range,  $t_c$  does not depend on the viscosity and reads  $t_c \sim (\ell_c^2 / \varepsilon)^{1/3}$ , where  $\varepsilon$  is the energy injected per unit mass. This leads us to define the dimensionless parameter that characterizes the competition between turbulent dispersion and compressibility effects at a given scale  $\ell_c$  by:

$$\Phi_C = \alpha \frac{\theta_0}{\ell_c^2} t_c. \quad (5)$$

We chose to define  $\Phi_C > 0$  for the attracting case which corresponds to  $\alpha \theta_0 > 0$ , and fixed  $\theta_0 = 1$  in all our DNS runs. Note that  $t_c$  is Kolmogorov-Obukhov phenomenological estimate of the time for which an eddy of the size of the scalar blob  $\ell_c$  survives in a turbulent flow.

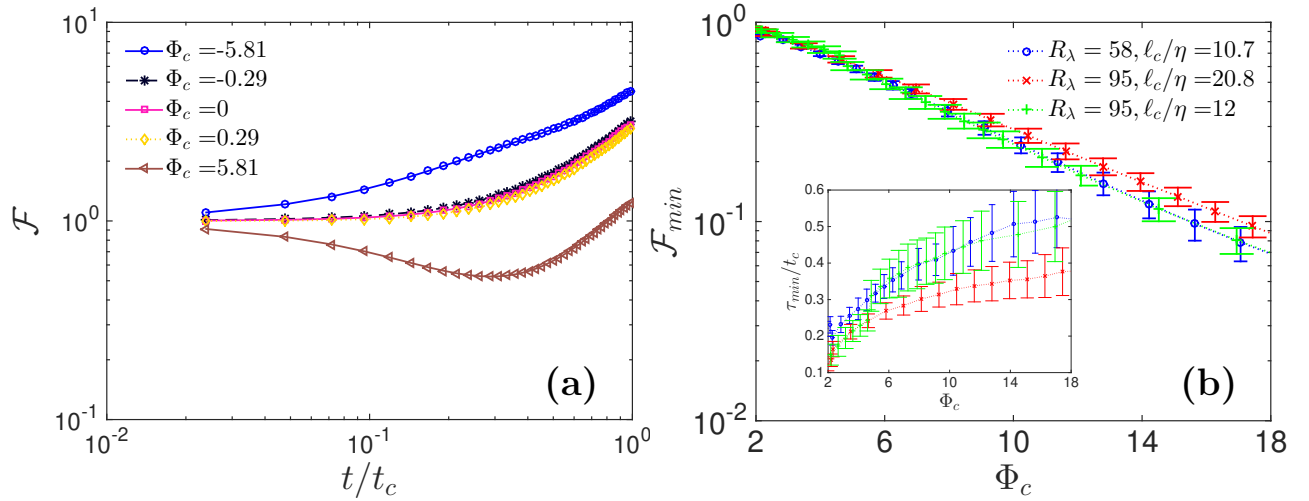


**Figure 3. Quantifying the de-mixing.** (a) Temporal evolution of the ratio of mean relative separation to its value at  $t = 0$ ,  $\mathcal{F}(t) \equiv r^2(t)/r^2(t = 0)$ , for different values of the dimensionless number  $\Phi_C$  characterizing the effective compressibility, from the DNS run with  $R_\lambda = 95$  and  $\ell_c/\eta = 20.8$ ;  $t_c$  is the time scale for which an eddy of size  $\ell_c$  survives in a turbulent flow. (b) Log-linear plots of minimum of  $\mathcal{F}$  versus  $\Phi_C$ .  $\mathcal{F}_{\min}$  is representative of the maximal de-mixing attained. Inset: Plots of  $\tau_{\min}$  versus  $\Phi_C$ , shows that the time to achieve maximum de-mixing (or contraction of the particle cloud) initially increases and then saturates at large values of  $\Phi_C$ .

### 3.2. Mixing and de-mixing of a turbulent cloud

In figure 2 we show the positions of two particle types at three different times: (a)  $t/t_c = 0$ , (b)  $t/t_c = 0.07$ , and (c)  $t/t_c = 0.22$ . These two particle types correspond to two different values of  $\Phi_C = 5.81$  (brown triangles,  $\alpha > 0$ ) and  $\Phi_C = -5.81$  (blue circles,  $\alpha < 0$ ). Starting at identical initial positions at  $t = 0$  (left), we observe that for  $\Phi_C > 0$  (brown triangles,  $\alpha > 0$ ) the particle cloud shrinks as a whole, whereas for  $\Phi_C < 0$  (blue circles,  $\alpha < 0$ ) the particles in the cloud move away from each other, resulting in an overall expansion.

To quantify the coherent expansion or the contraction of the particle cloud at short times, we measure the mean relative separation between the particles  $r(t)$  and its ratio to its value at  $t = 0$

$$\mathcal{F}(t) \equiv \frac{r^2(t)}{r^2(t = 0)}, \quad (6)$$

where  $r^2(t) = \langle (\mathbf{X}_i(t) - \mathbf{X}_j(t))^2 \rangle_{1 \leq i < j \leq N}$ . In order to get better statistics, 8 blobs of scalar containing particles are released at the same time with distances larger than half the box size. The simulation is then run and stopped before the different deformed blobs overlap. In figure 3 (a) we show the temporal evolution of  $\mathcal{F}$  for five different values of  $\Phi_C$  for the DNS run for which  $\ell_c/\eta = 20.8$  and  $R_\lambda = 95$ . The pink curve with squares represents the case of a pure tracer  $\Phi_C = 0$  ( $\mathcal{C} = 0$ ). For the phoretic particles with  $\Phi_C < 0$  (blue curves with circles and black curves with stars)  $\mathcal{F}$  increases faster than it

does for the pure tracers. This represents a case where the local environment selectively assists in the faster dispersal of these particles, thereby resulting in an enhanced mixing or expansion of the particle cloud at short times. In a direct contrast to this, for phoretic particles with  $\Phi_c > 0$  (yellow curve with diamonds and brown curve with triangles),  $\mathcal{F}$  first decreases until it reaches a minimum value and then it rises rapidly. This clearly represents a case of de-mixing aided by the local environment, whose extent depends on the value of  $\Phi_c$  and has been quantified in terms of the coherent contraction of the particle cloud monitored by measuring  $\mathcal{F}$ .

In the following, we focus on the case  $\Phi_c > 0$ , which results in de-mixing (see figure 3). We note that the lower the value reached by  $\mathcal{F}$ , the stronger is the de-mixing. We propose here a simple description of this effect, based on the standard Kolmogorov-Obukhov phenomenological theory of turbulence [20], resulting in a prediction of  $\mathcal{F}_{\min}$  as a function of  $\Phi_c$ .

We can use (3) and (4) to write

$$\frac{d\delta\mathbf{X}}{dt} = \delta\mathbf{u} + \alpha\delta\nabla\theta, \quad (7)$$

where  $\delta\mathbf{X}$  (resp.  $\delta\mathbf{u}$ ) is the difference between the positions (resp. velocities) of two phoretic particles (indices  $i, j$  have been dropped for the sake of simplicity). Note that the first term on the right hand side (RHS) in (7) is a velocity increment. In the absence of phoretic effect ( $\alpha = 0$ ), the term  $\delta\mathbf{u}$  is responsible for turbulent particle dispersion. This term averages to zero when the colloids are released, as the particle positions are *a-priori* not correlated with the flow velocity field [22]. At small times, this term contributes only a small correction to the constant term, in particular when  $|\Phi_c| \gtrsim 1$ , see figure 3. The second term is the phoretic contribution which produces the effect shown in figure 2 and 3. At a qualitative level, this term is smooth and nearly isotropic so that one has ( $t < t_c$ ,  $\delta\mathbf{X} \sim \delta\mathbf{X}_0$ )

$$\frac{d\langle\delta\mathbf{X}^2\rangle}{dt} \propto -\alpha\frac{\theta_0}{\ell_c^2}\langle\delta\mathbf{X}^2\rangle, \quad (8)$$

when averaging over particle pairs in the ballistic regime of turbulent dispersion. As long as the injected blob of scalar keeps its identity (with a simple, connected shape, before being torn apart by the turbulent flow), the compression experienced by the set of particles leads to the overall contraction of the cloud, given by:

$$2\ln\left(\frac{r}{r_0}\right) \propto -\Phi_c\frac{t}{t_c}. \quad (9)$$

The scalar blob retains its identity for a time  $\approx t_c$ , so the particle cloud keeps contracting for a time  $\approx t_c$ . During this time interval, the value of  $\mathcal{F}$  contracts by an amount, which increases with  $\Phi_c$ . Equation (9) suggests a simple relation between  $\mathcal{F}_{\min}$  and  $\Phi_c$ :

$$\mathcal{F}_{\min} \sim \tilde{\mathcal{F}}_0 \exp(-\gamma\Phi_c), \quad (10)$$

where  $\gamma$  is a constant *a-priori* of order 1. We emphasize that this prediction results from the competition between the contraction introduced by the scalar, and the mixing by the turbulent flow.



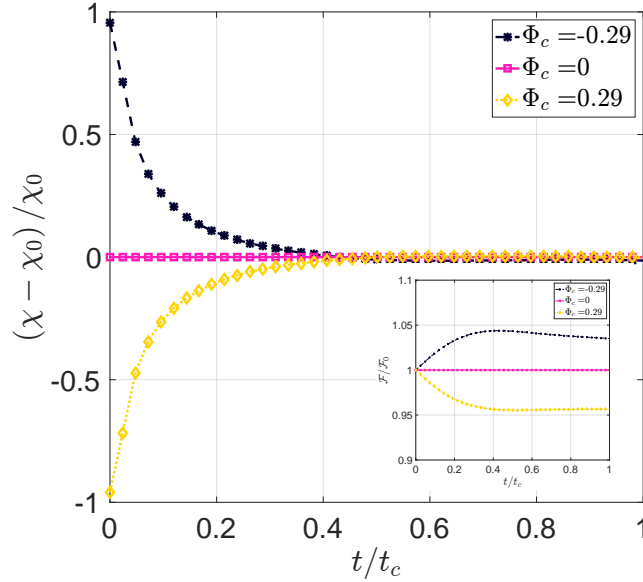


**Figure 4.** Dilatation factor  $\chi = \frac{1}{\mathcal{F}} \frac{d\mathcal{F}}{dt}$  and in the inset: Mean square separation in presence of phoresis normalized by the non-phoretic case; from the DNS run with  $R_\lambda = 95$  and  $\ell_c/\eta = 20.8$ .

We now turn to DNS runs to test the validity of this phenomenological prediction. In figure 3 (b) we plot  $\mathcal{F}_{\min}$  versus  $\Phi_c$  on log-linear scale for different particle cloud sizes and Reynolds numbers. We observe that for all the cases  $\mathcal{F}_{\min}$  decreases exponentially with increasing  $\Phi_c$ , as confirmed by straight lines on log-linear axes and whose slopes  $\gamma$  agree with each other within 15%. The inset of figure 3 (b) shows the plot of  $\tau_{\min}/t_c$  versus  $\Phi_c$  for the cases considered above. We notice that the time it takes to achieve maximum contraction of the particle cloud or the maximally de-mixed state for the phoretic particles has a tendency to saturate as  $\Phi_c$  increases. Moreover, we find that the particle cloud survives only for a fraction of time  $t_c$ . Our error bars are large, indicating a need for better statistical averaging; however, we believe that our conclusions will not change qualitatively.

As stressed in the introduction, the effect of phoresis on the transport properties of the particles can be best understood in terms of an effective compressibility. One way to characterize this compressibility, appropriate in the context of pair dispersion, is to introduce the dilatation factor :

$$\chi = \frac{1}{r^2} \frac{dr^2}{dt} = \frac{1}{\mathcal{F}} \frac{d\mathcal{F}}{dt}. \quad (11)$$

Figure 4 shows the dilatation factor  $\chi$  estimated for the smallest values of  $\Phi_c$  represented in figure 3; as it was difficult to see any measurable effect of phoresis in the latter. Figure 4 indicates that for values of  $\Phi_c \approx 0.3$ , the difference between  $\chi$  and the corresponding value in the case of a passive tracer,  $\chi_0$ , significantly deviates from 0. For completeness,

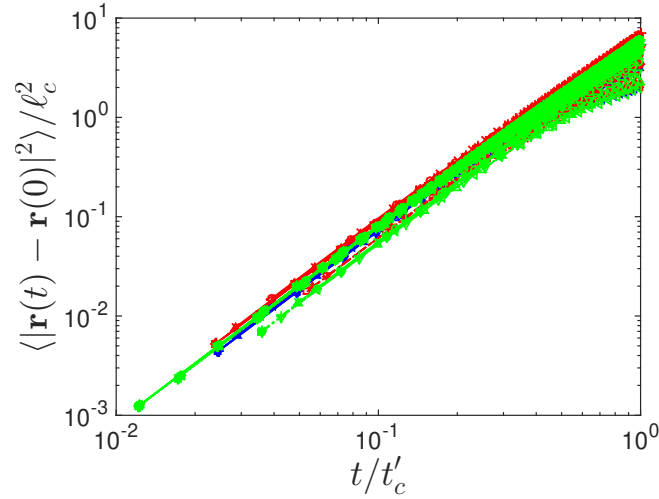


**Figure 5. Ballistic mean squared relative displacement at short times** Loglog plots of the mean-squared relative displacement  $\langle |\delta \mathbf{X}(t) - \delta \mathbf{X}(0)|^2 \rangle / \ell_c^2$  versus scaled time  $t/t'_c$ , where  $t'_c = t_c(1 + \beta \Phi_c^2)^{-\frac{1}{2}}$ , obtained from DNS runs for different values of  $\Phi_c$  (represented by different symbols) for three different values of Taylor-microscale Reynolds number  $Re_\lambda = 58$  (blue dashed lines  $\ell_c/\eta = 10.7$ ), 95 (red lines: dashed  $\ell_c/\eta = 20.8$  and colon  $(:)$   $\ell_c/\eta = 12.0$ ) and 175 (green lines: dashed  $\ell_c/\eta = 50.5$ , colon  $(:)$   $\ell_c/\eta = 30.3$  and dashed-dot  $\ell_c/\eta = 10.1$ ); different values of particle cloud size  $\ell_c$  is indicated by different line-types. In our simulations  $\Delta\theta = 1$  and  $t_c$  is time scale associated with  $\ell_c$ . See Table A2 for more details.

the values of  $\chi$  for all the values of  $\Phi_c$  in figure 3 are shown in figure A1, see Appendix A. It can be seen that even for values of  $\Phi_c = \mathcal{O}(10^{-1})$  the impact of phoresis on the initial dilation factor is of order one compared to the non-phoretic situation. The inset of figure 4, representing the ratio  $\mathcal{F}/\mathcal{F}_0$  then shows that although the dilation factor relaxes to the non-phoretic value in a timescale of a fraction of  $t_c$ , a sustained modification of the mean square pair separation of the order of 5% compared to the non-phoretic case does persist at timescales  $t \approx t_c$ . It can also be noted that these alternative ways of presenting the data better emphasize the symmetry between the compressing situation ( $\Phi_c > 0$ , showing a minimum of  $\mathcal{F}/\mathcal{F}_0$ , which was discussed earlier) and the dilating situation ( $\Phi_c < 0$ ), showing an equivalent maximum of  $\mathcal{F}/\mathcal{F}_0$ . Thus, a value of  $\Phi_c$  of order  $10^{-1}$  is sufficient to affect the rate of dilation of pairs of particles by a significant amount, albeit over a short time lapse. Yet, as suggested below, these effects may be prevalent in conditions where the scalar and the particles are in a steady state.

### 3.3. Short time separation of the particles in the cloud

To further understand the mixing and de-mixing process, we look at the two-particle statistics, where we compute how the relative separation between the particles changes with time. We again turn to phenomenological arguments to predict the behavior of

the mean-squared relative displacement at short-times

$$\begin{aligned}
\langle |\delta \mathbf{X}(t) - \delta \mathbf{X}(0)|^2 \rangle &\simeq \langle (\delta \mathbf{v})^2 \rangle t^2 \\
&\simeq [\langle (\delta \mathbf{u})^2 \rangle + \alpha^2 \langle (\delta(\nabla \theta))^2 \rangle] t^2 \\
&\simeq \frac{\ell_c^2}{t_c^2} (1 + \beta \Phi_c^2) t^2,
\end{aligned} \tag{12}$$

In going from the first to the second line in the above equation, we have neglected the cross term  $\langle \delta \mathbf{u} \cdot \delta(\nabla \theta) \rangle$ . This is justified by the complete lack of correlation between the injected scalar field  $\theta$  and the flow velocity  $\mathbf{u}$ . The dimensionless parameter  $\beta$  introduced in Eq. (12), is expected to be independent of  $\ell_c$  and  $Re_\lambda$ . Therefore, we can write

$$\langle |\delta \mathbf{X}(t) - \delta \mathbf{X}(0)|^2 \rangle / \ell_c^2 = A [t/t'_c]^2, \tag{13}$$

with  $t'_c = t_c(1 + \beta \Phi_c^2)^{-\frac{1}{2}}$  and  $A$  is a constant. In figure 5 we show the log-log plots of mean-squared relative displacement  $\langle |\delta \mathbf{X}(t) - \delta \mathbf{X}(0)|^2 \rangle / \ell_c^2$  versus scaled time  $t/t'_c$  for different values of  $\Phi_c$  (indicated by different symbols) for three different Reynolds numbers  $Re_\lambda = 58$  (blue lines),  $Re_\lambda = 95$  (red lines), and  $Re_\lambda = 175$  (green lines); and for different particle cloud sizes, see the caption of figure 5, as well as Table A1 and Table A2 in Appendix A for further details. These DNS runs confirm the phenomenological prediction that, when rescaled by the cloud size  $\ell_c$ , the mean-squared relative displacement is a linear function of  $(t/t'_c)^2$  in the ballistic regime. Moreover, we find that this statistical property is universal, as the plots for different  $\Phi_c$ ,  $Re_\lambda$  and  $\ell_c$  collapse onto each for  $\beta \simeq 0.05$ .

We end this section with a remark that in the present study we are interested in an elementary question, whether phoretic effects can lead to measurable consequences. For this reason, we focus on a simple quantity, namely the mean-square separation. However, much insight can be gained by systematically investigating the full distribution of separation at different times. Such an investigation will be the subject of future work.

#### 4. Discussion of the orders of magnitude: are phoretic effects observable ?

Whether phoretic effects (thermo- and diffusio-phoresis, in particular) can give rise to measurable effects is the important question that we address now. The present discussion is based on the parameter  $\Phi_c$ , introduced in (5), which has been demonstrated in simple problems, see Section 3, to provide a good way to quantify the importance of phoretic phenomena: The larger  $\Phi_c$  the larger the effect of phoresis.

##### 4.1. Revisiting the definition of $\Phi_c$

In terms of possible applications, two effects need to be taken into account when defining the parameter  $\Phi_c$ , relevant to evaluate the importance of phoretic effects.

First, the phoretic coefficient  $\alpha$  is generally found to depend on the local scalar field  $\theta$ , with a dependence of the form  $\alpha = D_p/\theta$ , where  $D_p$  has the dimension of a

diffusion coefficient [4, 5, 23]. This implies that the dimensionless expression of the flow compressibility, Eq. (5) simplifies to:

$$\Phi_C = D_p \frac{t_{lim}}{\ell_c^2}, \quad (14)$$

where  $\ell_c$  is the small length scale of the scalar  $\theta$  ( $\nabla^2 \theta \propto \theta/\ell_c^2$ ), and  $t_{lim}$  is the persistence time of the fluctuations of  $\theta$  inducing phoresis. In our problem, turbulence disrupts a blob of scalar of size  $\ell_c$ , in a time  $t_{lim}$  that depends on the  $\ell_c$ .

Second, whereas in studying phoretic effects in Section 3, we have explicitly considered scalars with a diffusion coefficient of the order of viscosity:  $Pr \approx 1$ , it should be kept in mind that in practice, the diffusion coefficient of the scalar can be significantly smaller than viscosity:  $Pr \approx 6$  in the case of thermophoresis, and  $Pr \approx 1000$  in the case of diffusiophoresis. We begin this section by discussing the parameter  $\Phi_C$  by taking into account the expression  $\alpha = D_p/\theta$ , and the large values of  $Pr$ .

The following discussion rests on the classical picture of the mixing of a scalar field by a turbulent flow. The fluctuations of the velocity field typically extend over a range of length scales, from the large (stirring) length,  $L$ , down to the Kolmogorov scale,  $\eta$ . A scalar field, advected by the flow, is also subject to molecular diffusion,  $\kappa \equiv \nu/Pr$ , where  $Pr$  is the Prandtl number already introduced. In applications with large Prandtl number the scalar fluctuations can extend down to scales much smaller than  $\eta$ . In fact, the smallest scale of the scalar fluctuations,  $\eta_B$ , known as the Batchelor scale, is of order  $\eta_B \equiv \eta Pr^{-1/2}$  for  $Pr \gg 1$  [24].

The persistence of scalar fluctuations at a scale  $\ell_c$  depends on the range of scale. Namely, when  $\eta \leq \ell_c \leq L$  (the size of the scalar blob lies in the inertial range), the blob is subject to the turbulent shear,  $\propto (\varepsilon/\ell_c^2)^{1/3}$ , so the persistent time is  $t_{lim} \propto (\ell_c^2/\varepsilon)^{1/3}$ . This is the case we have considered so far. In this case, the expression (14) reduces to

$$\Phi_C = \frac{D_p}{\nu} \left( \frac{\eta}{\ell_c} \right)^{4/3}. \quad (15)$$

which immediately shows that the largest possible value of  $\Phi_C$  is obtained when  $\ell_c \approx \eta$ :  $\Phi_C \lesssim D_p/\nu$ . In the other regime,  $\eta_B \leq \ell_c \leq \eta$ , the velocity field is smooth at the scale  $\ell_c$ , and the strain acting on a blob of size  $\ell_c$  is  $\propto (\varepsilon/\nu)^{1/2}$ . This implies that the time  $t_{lim} \propto (\nu/\varepsilon)^{1/2}$ , which is also known as the Kolmogorov time scale [20]. In this case, the expression for  $\Phi_C$  reduces to:

$$\Phi_C = \frac{D_p}{\ell_c^2} \times \left( \frac{\nu}{\varepsilon} \right)^{1/2} = \frac{D_p}{\nu} \times \left( \frac{\eta}{\ell_c} \right)^2 = \frac{D_p}{\kappa} \times \left( \frac{\eta_B}{\ell_c} \right)^2 \quad (16)$$

Eq. 16 shows that the value of  $\Phi_C$  can vastly exceed  $D_p/\nu$ , the limiting value when  $\ell_c \geq \eta$ . Specifically, in the case of blobs of size  $\ell_c \approx \eta_B$ ,  $\Phi_C \approx D_p/\kappa$ . These expressions are particularly relevant, given the large values of  $Pr$  in the relevant cases of thermo- and diffusiophoresis.

To summarize, the estimates given so far show that the maximum strength of the phoresis effects quantified in terms of the parameter  $\Phi_C$  can be ultimately expressed as

ratio of the diffusion coefficient  $D_p$  and either the viscosity  $\nu$  or the diffusion coefficient of the scalar field (temperature or salt)  $\kappa$ .

#### 4.2. How large are phoretic effects ?

To proceed, we use the values of  $D_p$  reported in the literature. Microfluidic experiments have shown so far a maximum effect when using carboxylate colloids in gradients of Lithium Chloride (LiCl), this combination of particle and salt lead to a diffusiophoretic coefficient as large as  $D_p \approx 300\mu\text{m}^2\text{s}^{-1}$ . In experiments on thermophoresis values of  $D_p$  as large as  $3000\mu\text{m}^2\text{s}^{-1}$  have been measured [23], hence 10 times larger than in the diffusiophoresis case. These estimates are consistent with those measured in the oceans [25].

This implies that the ratio  $D_p/\nu$ , which corresponds to the largest possible value of  $\Phi_C$  when  $\ell_c$  is in the inertial range, see (15), is of the order  $10^{-4}$  in the case of diffusiophoresis, and of order  $3 \times 10^{-3}$  in the case of thermophoresis.

These values are clearly smaller than the values necessary to measure any of the effects discussed in Section 3. Assuming, however, a value of  $\ell_c$  smaller than  $\eta$ , but larger than  $\eta_B$  shows that the values of  $\Phi_C$  cannot be larger than  $\Phi_C \lesssim 0.02$  in the case of thermophoresis, and  $\Phi_C \lesssim 0.1$  in the case of diffusiophoresis. These values are sufficient to observe, in principle, a significant effect of diffusiophoresis.

It is useful to compare the previous estimates with existing experimental results, where effects of phoresis were unambiguously found.

In the microfluidic experiments on diffusiophoresis by Abecassis *et al.* [4, 5], using a laminar flow, the limiting time is given by the mean advection  $t_{lim} = z_{obs}/U_0$  (where  $z_{obs}$  is the observation position along the micro-channel and  $U_0$  is the advection velocity along the channel. Interestingly,  $\Phi_C$  in their experiment can then be estimated to be in the range  $[10^{-3} - 10^{-1}]$ , with measurable effects on the spreading and focusing of the concentration profile of an initial colloidal band.

For the experiments in chaotic flows by Desseigne *et al.* [6] and Mauger *et al.* [8], which are closer in spirit to the present work, the limiting time scale at the early stage of the process is given by the period of the chaotic cycle (at larger times the diffusion time of salt also becomes important), leading to typical values of  $\Phi_C$  of the order of  $[10^{-3} - 10^{-2}]$ , with subtle but still measurable effects on the concentration field of colloids and its gradients. We also notice that Schmidt *et al.* [17] report a possible observation of diffusiophoresis, by looking at clustering properties of particles at inertial scales in a turbulent gravity flow with salt gradients. In such conditions, the largest expected value for  $\Phi_C$  is of the order of  $D_p/\nu$  (with  $\nu$  the kinematic viscosity of the fluid), which in their experiment is of the order of  $10^{-4}$ .

It is worth pointing out that in the problem of pair dispersion, as we have studied it numerically, the initial scalar distribution affects colloid transport for a small time only. Scalar gradients, in a statistically steady-state regime, may act cumulatively, resulting in much larger effects. As such, the requirement in term of  $\Phi_C$  to observe a significant

phoretic effect could be conceivably much reduced, compared to what we found in the purely transient problem investigated here.

The above discussion and the values of  $\Phi_C$  obtained on the basis of [23, 25] indicate that the phoretic effects can be important and therefore may affect the transport of small organisms, or pollutant particles, as a result of local gradients of salinity, dissolved oxygen, temperature, etc.

## 5. Summary

In this work, we have explored the interplay between turbulent transport and phoretic effects. The specific problem investigated is purely transient, and concerns a cloud of colloids, released with a blob of scalar of size  $\ell_c$  in an otherwise statistically stationary flow.

The phenomena discussed here results from a competition between the compressibility of the particle velocity field, (3), and the fast dispersion of the scalar blob. On dimensional grounds, this competition can be described at short times by the dimensionless ratio  $\Phi_C$ , defined by (5).

In the case where the scalar generates an effective compressibility ( $\Phi_C > 0$ ), we observed that particles tend to come together, over a time which is a fraction of the time  $t_c$ , characteristic of the size  $\ell_c$ . The minimum in the mutual distance between particles can be approximated as a function of  $\Phi_C$ , which decays exponentially at large values of  $\Phi_C$ . The quantity  $\Phi_C$  provides a satisfactory way to describe the initial stage of the separation between particles.

We have used our numerical results, as well as those from previous studies, to discuss the significance of the approach followed in the present study for the existing or possible experiments and the natural flows. The discussion of the previous section indicates that in order to maximize the chances to observe a signature of diffusiophoresis at inertial scales of turbulence, one has to: (i) use an appropriate indicator (e.g., the dilation factor for pair separation diagnosis) and (ii) maximize  $D_p$  and minimize both  $\epsilon$  and the observation scale  $\ell_c$ .

We conclude by recalling that the present study has been focused on the transient problem, where the scalar field is injected together with the particles.

In this time-dependent problem, the colloid velocity field is either manifestly attracting or repelling, possibly leading to the strong mixing or de-mixing effects, illustrated in figures 2 and 3. Such strong effects are not expected when colloids are injected in a scalar field in a statistically steady state, as the divergence of the colloid velocity field  $\nabla \cdot \mathbf{v}$ , is equally likely to be positive or negative. The related but distinct problem of the properties of the colloid distribution in the presence of a of turbulent scalar field in a steady state therefore deserves further attention. In fact, as it is the case in the problem of inertial particles in a turbulent flow [26, 13, 15], the compressibility of the velocity field experienced by the particles is likely to lead to preferential concentration. It will be interesting to explore the analogies and differences

	$N_c$	$\nu \times 10^{-3}$	$\kappa \times 10^{-3}$	$R_\lambda$	$u_{rms}$	$L_0$	$\lambda$	$\eta$	$k_{max}\eta$	$\epsilon$	$\ell_c/\eta$	$\beta$
Run1	96	7.5	15.0	58	0.728	1.38	0.596	0.04	1.79	0.168	10.7	0.05
Run2	192	3.0	6.0	95	0.7289	1.30	0.39	0.0204	1.83	0.157	20.8	0.05
Run3	192	3.0	6.0	95	0.7289	1.30	0.39	0.0204	1.83	0.157	12.0	0.05
Run4	384	0.94	1.88	175	0.75	1.23	0.22	0.0084	1.52	0.168	50.5	0.05
Run5	384	0.94	1.88	175	0.75	1.23	0.22	0.0084	1.52	0.168	30.3	0.06
Run6	384	0.94	1.88	175	0.75	1.23	0.22	0.0084	1.52	0.168	10.1	0.07

**Table A1.** Parameters for the DNS runs **Run1** – **Run6**:  $N_c^3$  the number of collocation points,  $\nu$  the viscosity,  $\kappa$  the diffusivity,  $R_\lambda = u_{rms}\lambda/\nu$  the Taylor-scale based Reynolds number,  $u_{rms} = \sqrt{2E/3}$  the root-mean-squared velocity and  $\lambda = u_{rms}/\sqrt{\langle(\partial_x u)^2\rangle}$  the Taylor-microscale,  $L_0 = (\pi/2u_{rms}^2) \sum_k E(k)/k$  the integral length scale,  $\eta = (\nu^2/2\Omega)^{1/4}$  the Kolmogorov dissipation length scale,  $\epsilon$  the energy injection rate, and  $\ell_c$  the measure of size of the Gaussian scalar blob.  $E$  is the mean kinetic energy and  $\langle(\partial_x u)^2\rangle = 2\Omega/15$ , where  $\Omega$  is the enstrophy. In our DNSs we have fixed the Prandtl number  $Pr = \nu/\kappa$  at 0.5.

between the two problems, in particular in terms of particle dispersion properties [27, 28].

**Acknowledgements:** We are very thankful to C. Cottin-Bizonne, F. Raynal and C. Ybert for their insight into the physics of phoretic mechanisms. V.S. also thanks D. Buaria for useful discussions. This work was supported by the European project EuHIT - European High-performance Infrastructures in Turbulence, and by French research programs ANR-16-CE30-0028 and LABEX iMUST (ANR-10-LABX-0064) of Université de Lyon, within the program “Investissements d’Avenir” (ANR-11-IDEX-0007).

## Appendix A. Supplementary information on the DNS runs

This appendix presents a list of the flows we have simulated (Table A1), and of the values of  $\alpha$  and  $\Phi_C$  used (Table A2).

In addition, figure A1 presents the values of  $\chi$  and of the mean separation  $\mathcal{F}/\mathcal{F}_0$  for values of  $\Phi_C$  larger than those shown in figure 4 of the main text.

## References

- [1] Anderson J L 1989 *Ann. Rev. Fluid Mech.* **21** 61–99
- [2] Li D 2008 *Encyclopedia of microfluidics and nanofluidics* (Springer Science & Business Media)
- [3] Zborowski M and Chalmers J J 2015 *Wiley Encyclopedia of Electrical and Electronics Engineering*
- [4] Abécassis B, Cottin-Bizonne C, Ybert C, Ajdari A and Bocquet L 2008 *Nature materials* **7** 785–789
- [5] Abecassis B, Cottin-Bizonne C, Ybert C, Ajdari A and Bocquet L 2009 *New J. Phys.* **11** 075022
- [6] Deseigne J, Cottin-Bizonne C, Stroock A D, Bocquet L and Ybert C 2014 *Soft matter* **10** 4795–4799
- [7] Volk R, Mauger C, Bourgoïn M, Cottin-Bizonne C, Ybert C and Raynal F 2014 *Physical Review E* **90** 013027

$\Phi_C$					$\Phi_C$			
<i>Symbol</i>	$\alpha$	Run1	Run2	Run3	$\alpha$	Run4	Run5	Run6
○	−1.0	−5.69	−5.81	−12.10	−0.1	−0.569	−1.12	−4.86
X	−0.5	−2.84	−2.91	−6.05	−0.075	−0.43	−0.84	−3.65
+	−0.1	−0.57	−0.58	−1.21	−0.05	−0.28	−0.56	−2.43
*	−0.05	−0.28	−0.29	−0.60	−0.01	−0.057	−0.11	−0.47
□	0	0	0	0	0	0	0	0
◇	0.05	0.28	0.29	0.60	0.01	0.057	0.11	0.49
▽	0.1	0.57	0.58	1.21	0.05	0.28	0.56	2.43
△	0.5	2.84	2.91	6.05	0.075	0.43	0.84	3.65
◁	1.0	5.69	5.81	12.10	0.1	0.57	1.12	4.86

**Table A2.** Values of the dimensionless number  $\Phi_C$  from our DNS runs Run1–Run6 for nine different values of  $\alpha$ . The symbols in the first column serve as guide for the curves in figure 5.

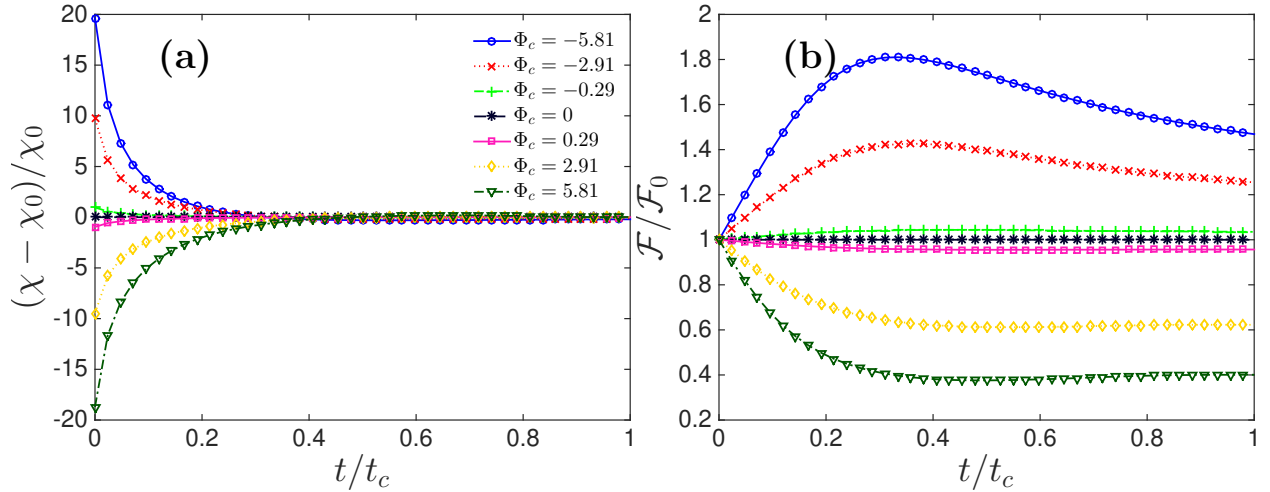


**Figure A1.** (a) Dilatation factor  $\chi = \frac{1}{\mathcal{F}} \frac{d\mathcal{F}}{dt}$  and (b) mean square separation in presence of phoresis normalized by the non-phoretic case, from the DNS run with  $R_\lambda = 95$  and  $\ell_c/\eta = 20.8$ .

- [8] Mauger C, Volk R, Machicoane N, Bourgoïn M, Cottin-Bizonne C, Ybert C and Raynal F 2016 *Phys. Rev. Fluids* **1**(3) 034001
- [9] Shaw R 2003 *Ann. Rev. Fluid Mech.* **35** 183–227
- [10] Balachandar S and Eaton J K 2010 *Ann. Rev. Fluid Mech.* **42** 111–133
- [11] Maxey M R and Riley J J 1983 *Phys. Fluids* **26** 883–889
- [12] Gatignol R 1983 *J. Méc. Théor. Appl.* **1** 143–160
- [13] Balkovsky E, Falkovich G and Fouxon A 2001 *Phys. Rev. Lett.* **86** 2790–2793
- [14] Falkovich G, Fouxon A and Stepanov M G 2002 *Nature* **419** 151–154
- [15] Falkovich G and Pumir A 2004 *Phys. Fluids* **16** L47–50
- [16] Belan S, Fouxon I and Falkovich G 2014 *Phys. Rev. Lett.* **112**(23) 234502
- [17] Schmidt L, Fouxon I, Krug D, van Reeuijck M and Holzner M 2016 *Phys. Rev. E* **93**(6) 063110



- [18] De Lillo F, Cencini M, Musacchio S and Boffetta G 2016 *Physics of Fluids* **28** 035104
- [19] Mitra D, Haugen N E L and Rogachevskii I 2016 *arXiv preprint arXiv:1603.00703*
- [20] Frisch U 1995 *Turbulence* 1st ed (Cambridge University Press) ISBN 0 521 45713 0
- [21] Pumir A 1994 *Phys. Fluids* **6** 2118–2132
- [22] Bragg A D and Collins L R 2014 *New J. Phys.* **16** 055013
- [23] Vigolo D, Rusconi R, Stone H A and Piazza R 2010 *Soft Matter* **6** 3489 ISSN 1744-683X
- [24] Batchelor G K 1959 *J. Fluid Mech.* **5** 113–133
- [25] Thorpe S A 2005 *The turbulent ocean* 1st ed (Cambridge University Press) ISBN 13 978-0-521-83543-5
- [26] Maxey M R 1983 *J. Fluid Mech.* **174** 441–465
- [27] Bec J, Biferale L, Lanotte A S, Scagliarini A and Toschi F 2010 *J. Fluid Mech.* **645** 497–528
- [28] Bragg A D, Ireland P J and Collins L R 2016 *Phys. Fluids* **28** 013305